

Stroke

American Stroke
AssociationSM

JOURNAL OF THE AMERICAN HEART ASSOCIATION

A Division of American
Heart Association



Roles of Inflammation and the Activated Protein C Pathway in the Brain Edema Associated With Cerebral Venous Sinus Thrombosis

Mutsumi Nagai, Satoshi Terao, Gokhan Yilmaz, Cigdem E. Yilmaz, Charles T.
Esmon, Eiju Watanabe and D. Neil Granger

Stroke 2010;41;147-152; originally published online Nov 5, 2009;

DOI: 10.1161/STROKEAHA.109.562983

Stroke is published by the American Heart Association, 7272 Greenville Avenue, Dallas, TX 75214
Copyright © 2010 American Heart Association. All rights reserved. Print ISSN: 0039-2499. Online
ISSN: 1524-4628

The online version of this article, along with updated information and services, is
located on the World Wide Web at:

<http://stroke.ahajournals.org/cgi/content/full/41/1/147>

Subscriptions: Information about subscribing to Stroke is online at
<http://stroke.ahajournals.org/subscriptions/>

Permissions: Permissions & Rights Desk, Lippincott Williams & Wilkins, a division of Wolters
Kluwer Health, 351 West Camden Street, Baltimore, MD 21202-2436. Phone: 410-528-4050. Fax:
410-528-8550. E-mail:
journalpermissions@lww.com

Reprints: Information about reprints can be found online at
<http://www.lww.com/reprints>

Roles of Inflammation and the Activated Protein C Pathway in the Brain Edema Associated With Cerebral Venous Sinus Thrombosis

Mutsumi Nagai, MD, PhD; Satoshi Terao, MD; Gokhan Yilmaz, MD; Cigdem E. Yilmaz, MD, PhD; Charles T. Esmon, PhD; Eiju Watanabe, MD, PhD; D. Neil Granger, PhD

Background and Purpose—Increased blood–brain barrier (BBB) permeability, brain edema, and hemorrhage are important consequences of cerebral venous sinus thrombosis (CVST). The objective of this study was to define the role of the protein C pathway in the BBB permeability and edema elicited by experimental CVST. The role of neutrophil recruitment was also evaluated.

Methods—Edema, BBB permeability, leukocyte–endothelial cell adhesion (LECA) and inflammatory cytokine levels were monitored in a murine model of CVST. The role of activated protein C (APC) was assessed in wild type mice (WT) receiving APC neutralizing antibody and in endothelial protein C receptor overexpressing mice (EPCR-tg). Neutrophil involvement was evaluated using an anti-CD18 antibody (Ab) and antineutrophil serum.

Results—Brain edema and increases in BBB permeability and LECA were noted 48 hours after CVST. APC immunoblockade exacerbated these responses, while EPCR-tg exhibited blunted responses, as did WT treated with either antineutrophil serum or the CD18 Ab.

Conclusions—The protein C pathway protects the brain against the deleterious microvascular responses to CVST, a response that appears to be linked to the recruitment of inflammatory cells. (*Stroke*. 2010;41:147-152.)

Key Words: endothelial protein C receptor ■ activated protein C ■ brain edema
■ blood–brain barrier ■ leukocyte adhesion

Cerebral venous sinus thrombosis (CVST) is frequently associated with coagulation disorders (eg, protein C [PC] deficiency) and systemic inflammatory diseases (eg, sepsis).¹ Blood–brain barrier (BBB) dysfunction and the resultant edema and hemorrhage, and an elevated intracranial pressure have all been implicated in the injury that accompanies CVST in human brain.^{2,3} Experimental models of CVST have also revealed that BBB disruption and infiltration of inflammatory cells occurs in proximity to the site of thrombosis.^{4–7} Although severe brain edema is known to be a poor prognostic indicator for CVST, the mechanisms that elicit this deleterious response remain undefined. It is also unclear whether chemical signals generated during the thrombogenic response or the resultant inflammatory response contributes to the brain edema and BBB alterations after CVST.

Activated PC (APC) is produced by endothelial cells via the interaction of PC with thrombin–thrombomodulin complex and the endothelial cell protein receptor (EPCR).^{8–10} The pathophysiological role of the PC pathway in CVST may extend beyond the thrombogenic process. APC has recently

been shown to exert antiinflammatory, vasculoprotective, and neuroprotective effects in animal models of ischemic and hemorrhagic stroke.^{11–20} Although CVST is considered a form of stroke, ischemia does not appear to be an initiating event in this condition.¹⁰ Hence, it remains unclear whether APC can exert similar vasculoprotective effects in the brain after CVST.

The objective of this study was to determine whether genetic or immunologic manipulation of the PC pathway alters the brain injury response to CVST. To this end, brain water content (edema), BBB permeability, and leukocyte–endothelial cell adhesion were monitored at 3 and 48 hours after the induction of CVST in mice. Our findings support a role for the PC pathway and inflammatory cells in the brain edema associated with CVST.

Materials and Methods

Animal Preparation

Male C57BL/6 (WT; n=151, Jackson Laboratories, Bar Harbor, Me) and transgenic mice overexpressing EPCR (EPCR-tg; n=11) were

Received July 15, 2009; final revision received September 2, 2009; accepted September 9, 2009.

From the Department of Molecular and Cellular Physiology (M.N., S.T., G.Y., C.E.Y., D.N.G.), Louisiana State University Health Sciences Center, Shreveport; the Cardiovascular Biology Research Program (C.T.E.), Oklahoma Medical Research Foundation, Oklahoma City; and the Howard Hughes Medical Institute; and the Department of Neurosurgery (E.W.), Jichi Medical University, Tochigi, Japan.

Correspondence to D. Neil Granger, PhD, Department of Molecular and Cellular Physiology, Louisiana State University Health Sciences Center, 1501 Kings Highway, Shreveport, LA 71130. E-mail dgrang@lsuhsc.edu

© 2009 American Heart Association, Inc.

Stroke is available at <http://stroke.ahajournals.org>

DOI: 10.1161/STROKEAHA.109.562983

used. The EPCR-tg (backcrossed into WT mice) exhibit normal size, weight, viability, fertility, blood cell count, and chemistries as described.²¹ EPCR protein levels in all organs of the transgenic mice are at least 8-fold higher than in WT. All experimental procedures involving the use of animals were reviewed and approved by the Institutional Animal Care and Use Committee of LSU Health Sciences Center and performed according to the criteria outlined by the National Institutes of Health.

Induction of Cerebral Venous Sinus Thrombosis

Each mouse was anesthetized by intraperitoneal injection of ketamine hydrochloride (100 mg/kg) and xylazine (10 mg/kg). A longitudinal craniotomy (5 mm × 1 mm) was performed between the bregma and lambda, producing a narrow window lying just above the superior sagittal sinus (SSS). Previously reported models of SSS thrombosis used filter paper strips soaked with FeCl₃ that were placed over the SSS.^{4,6,22,23} We found that it is difficult to prevent direct contact of the filter paper with the brain surface, which results in FeCl₃-induced necrosis and inflammation in adjacent cortical tissue. In this study, SSS thrombosis was induced without injury to cortical tissue by direct topical placement of a 5-mm length of 6-0 silk thread soaked with 20% FeCl₃ (Sigma-Aldrich) on the sinus for a 5- to 10-minute period in the absence of light. At the 5-minute period, the field was washed with warmed normal saline after removing the thread and checked thrombus formation. If the initial procedure did not produce enough thrombus for complete occlusion (occurred in approximately 30% to 50% of mice), 5 minutes more FeCl₃ attachment was repeated (which yielded an occluding thrombus in 100% of mice). In sham animals, a saline-soaked silk thread was placed topically on the SSS. Cerebral blood flow in the parietal cortex was measured before and after CVST induction using a laser Doppler flowmeter (ML191 Blood Flow Meter, AD Instruments). On completion of the thrombosis (or sham) protocol, the window was closed and the animal was allowed to recover in its cage, where it had free access to food and water. Two days later, the mice were studied (as described below) under anesthesia and then euthanized by anesthetic overdose after data/sample collection. Preliminary experiments confirmed that blood pressure and blood gases were not affected by the surgical procedure.

Experimental Protocols

Time-dependent changes in brain edema and inflammation were monitored in mice subjected to CVST (or a sham procedure) and then allowed to recover for either 3 or 48 hours. Brain edema, BBB permeability, leukocyte–endothelial cell adhesion, and cytokine levels were monitored. The role of the PC pathway was evaluated (at 48 hours after CVST induction) in 3 groups: (1) control WT (WT-cont), (2) WT receiving (i.v.) 40 μg of rat antimouse APC monoclonal antibody (MPC1609; Oklahoma Medical Research Foundation) 20 minutes before CVST induction (WT-APC Ab), and (3) EPCR-tg. The contribution of leukocytes to the increased BBB permeability and brain edema was evaluated (at 48 hours after CVST induction) in WT receiving either a rat antimouse CD18 monoclonal antibody (GAME-46; BD Biosciences; CD18Ab) or mouse antineutrophil serum (RB6–8C5, Accurate Chemical; ANS). Two doses (30 μg each) of the CD18Ab were administered intravenously 15 minutes before CVST induction and 24 hours thereafter (WT-CD18Ab). The blocking effect of the CD18Ab was verified by monitoring leukocyte adhesion in treated versus untreated mice. The ANS was administered (150 μg) intraperitoneally 24 hours before CVST to deplete circulating neutrophils²⁴ (WT-ANS). Neutrophil depletion (from 4600 ± 1174 to 440 ± 167/mm³ cells) was verified by counting neutrophils in peripheral blood before ANS injection and immediately before the experiment. These groups were compared with the WT-control group. To address potential nonspecific effects of antibody administration, 7 WT-control mice received an equal dose of control antibody (Rat IgG1 Isotype Control, R & D Systems). In these mice, brain water content (78.77 ± 0.06 versus 78.87 ± 0.13) and survival rate did not differ from WT-control mice not receiving the control antibody.

Brain Water Content

At 48 hours after CVST induction, the brain was removed and stripped of the dura mater, brain stem, and cerebellum. The cerebrum was placed into a 70°C oven for 4 days. The water content was determined from the formula [(wet brain weight – dry brain weight)/wet brain weight] and expressed as percent.

Intravital Videomicroscopy

The cerebral microcirculation was examined with an upright fluorescent microscope for measurements of BBB permeability and leukocyte–endothelial cell adhesion. The vessels studied were approximately 3 mm from the site of SSS thrombosis. The microscope was equipped with filter cubes for green and blue fluorescence. The microscopic images were captured with a video recorder timer (Panasonic Japan, WJ-810; Panasonic Japan).

BBB Permeability

A modification of the procedure of Yuang et al was used to quantify BBB permeability, with FITC-dextran (40 kDa; Sigma-Aldrich) as the tracer molecule.^{25,26} A cranial window (3 mm diameter) was created 3 mm lateral and 2.5 mm posterior to the bregma. The dura mater was removed, the brain surface was immersed in artificial CSF, and the window closed with a cover slip. FITC-dextran was injected into the femoral vein (10 mg/mL, 1 mL/kg), and 30 s thereafter the brain microvasculature was illuminated for 30 s, followed by 1-s illumination every 30 s for 4 minutes and then 1 s every minute for 10 minutes (to minimize the photochemical injury).

Images of FITC fluorescence were recorded, transferred to a personal computer with ImageJ software (National Institutes of Health), and analyzed off-line. A 10 × 50-μm rectangular region of interest (ROI) was selected within a venule and a corresponding ROI was selected outside the vessel, within 10 μm of the vessel wall. The ROI values used to estimate BBB permeability in each animal were averaged from 3 vessels. Permeability was calculated using the formula:

$$P = (1 - H_{ct}) 1/I_v \times V/S \times dI_t/dt$$

where, I_t is tissue fluorescence intensity, I_v is initial fluorescence intensity within the vessel, V/S is the ratio of vessel volume and surface area, and H_{ct} is hematocrit (set at 45%). After subtracting the rate of change of the background intensity, dI_t/dt was determined from the slope of the tissue pixel intensity versus time curve obtained between 30 s and 5 minutes after tracer injection.

Leukocyte–Endothelial Cell Adhesion

On completion of the FITC-dextran permeability measurements, the mice received 50 μL of 0.02% rhodamine 6G (Sigma Chemical) to label circulating leukocytes. Leukocyte–endothelial cell adhesion was observed in randomly selected venular segments (25 to 45 μm diameter and 100 μm length). Adherent leukocytes remained stationary within the venule for a period ≥ 30 s and were normalized to venule surface area.

Cytokine Levels

A cytometric bead array (CBA Mouse Inflammation Kit, BD Biosciences) was used to measure the concentration of interleukin-12, TNF-α, interferon-gamma, monocyte chemoattractant protein-1 (MCP-1), interleukin-10 (IL-10), and interleukin-6 in plasma and brain tissue. Samples were collected at either 3 or 48 hours after CVST induction or a sham procedure. A group of mice not exposed to any surgical procedure (control) was also evaluated. Cytokine concentrations in the sham and CVST groups were expressed as pg/g (brain weight) or pg/mL (plasma) and normalized to the values measured in the control (no surgery) group.

Statistical Analyses

All data were expressed as mean ± SE. Statistical difference ($P < 0.05$) between the different groups was determined by a 1-way analysis of variance (ANOVA) with the Fisher post hoc test or Student t test. A 2-way ANOVA was used to determine time-dependent differences in

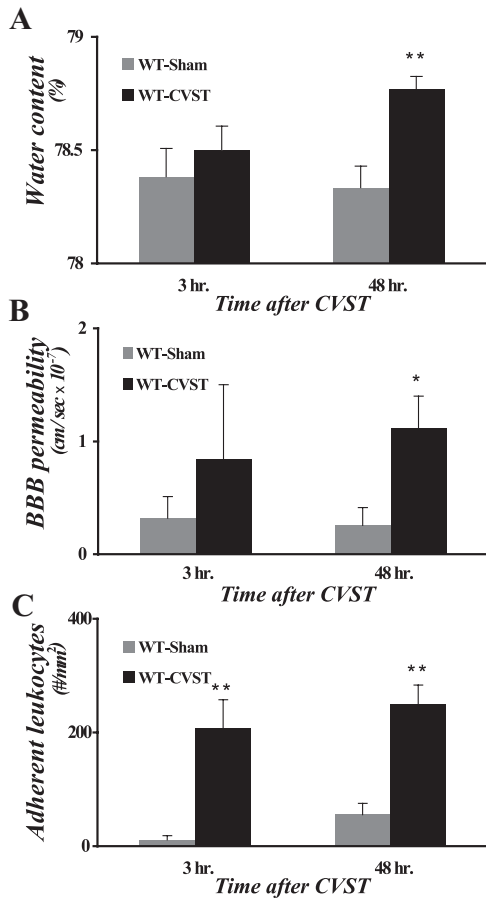


Figure 1. Time-dependent changes in brain water content, BBB permeability, and leukocyte-endothelial cell adhesion after CVST. In WT-Sham-3 hour, WT-CVST-3 hour, WT-Sham-48 hour, WT-CVST-48 hour, n=5, 5, 5, 8, respectively, in A, whereas n=5, 5, 5, 6 in B and C. ***P*<0.01, **P*<0.05 vs sham group.

cytokine concentration. Mortality rates were compared with a χ^2 test. All analyses were performed using Stat View 4.5 software (Abacus Concepts Inc).

Results

Blood Flow Changes

The reduction of cerebral blood flow after the induction of CVST in WT (n=5) was $9.4 \pm 5.0\%$, which was not statistically significant from the pre-CVST value.

Time-Dependent Changes in Brain Water Content and Inflammation

Figure 1 summarizes the time-dependent changes in brain water content, BBB permeability, and adherent leukocytes in cerebral venules of WT subjected to either CVST or a sham procedure (controls). At 3 hours after CVST, brain water content (Figure 1A) and BBB permeability (Figure 1B) were not significantly different from control values. However, a large increase in the number of adherent leukocytes (Figure 1C) was noted in venules of CVST exposed mice. At 48 hours, significant brain edema was detected and there was a corresponding increase in BBB permeability. The number of

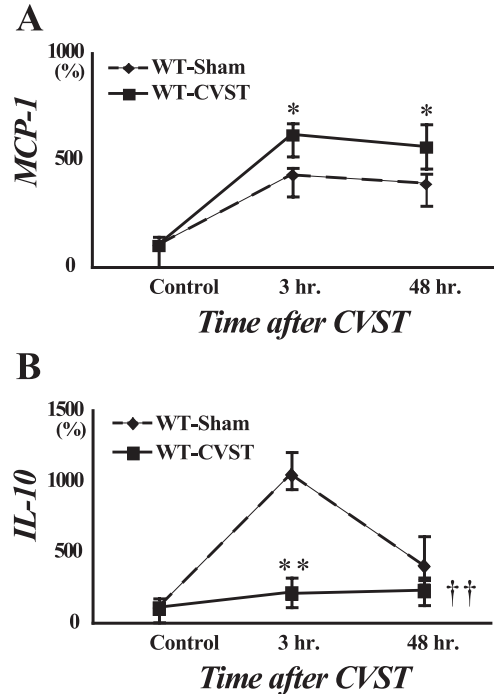


Figure 2. Changes in brain levels of MCP-1 and IL-10 after CVST. Mice per group in Control, WT-Sham-3 hour, WT-CVST-3 hour, WT-Sham-48 hour, WT-CVST-48 hour were n=10, 11, 9, 10, 10 in A and B. **P*<0.05, ***P*<0.01 vs sham group at each time point. ††*P*<0.01 two-way ANOVA for entire time-course between 2 groups.

adherent leukocytes remained significantly elevated at 48 hours.

Of the 6 cytokines monitored in brain tissue and plasma after CVST, only MCP-1 and IL-10 levels in brain tissue were significantly altered. MCP-1 concentration in brain began to rise (compared to sham controls; Figure 2A) and IL-10 level began to fall at 3 hours after CVST (Figure 2B). Plasma cytokines levels were not altered by CVST.

Role of the PC

Figure 3 compares the changes in brain water content, BBB permeability, and number of adherent leukocytes observed at 48 hours after CVST between WT-cont, WT-APC Ab, and EPCR-tg. The EPCR-tg exhibited a significant attenuation of CVST-induced brain edema (Figure 3A). Treatment with the APC Ab tended to augment brain water content, although this did not achieve statistical significance. The WT+APC Ab group also exhibited a mortality rate of 38.5% (5 of 13 mice), whereas all other CVST groups exhibited 0% mortality, with 8 of 8 (WT-cont) and 6 of 6 (EPCR-tg) surviving (*P*<0.05).

The increased BBB permeability elicited by CVST was greatly exaggerated in mice treated with the APC Ab and significantly attenuated in the EPCR-tg (Figure 3B). A similar pattern was noted for recruitment of adherent leukocytes in cerebral venules (ie, increased adhesion with APC Ab), and an attenuated response in EPCR-tg (Figure 3C).

Role of Leukocytes

The data from the different experimental groups were used to examine the relationship between BBB permeability and

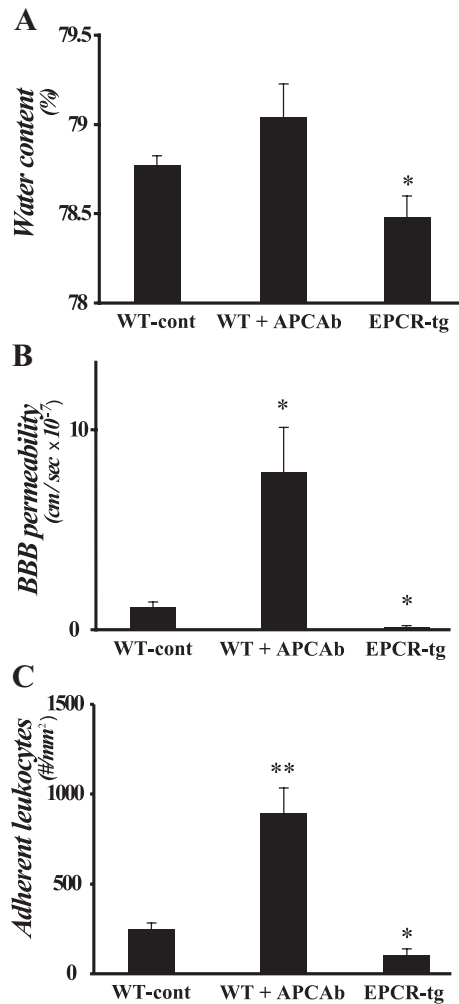


Figure 3. CVST-induced responses at 48 hours after manipulation of the protein C pathway. WT mice that were exposed to CVST induction (by FeCl₃) 48 hours before the measurements, but without any treatment. In WT-cont, WT+APCAb, and EPCR-tg, n=8, 8, 6, respectively in A, whereas n=6, 6, 5 in B and C. *P<0.05, **P<0.01 vs WT.

leukocyte adherence in cerebral venules (Figure 4). This analysis revealed a significant positive correlation between the 2 variables, suggesting that the protective effects of the APC-directed interventions on BBB permeability may relate to their ability to blunt leukocyte adhesion. To directly address this possibility, we determined whether interfering

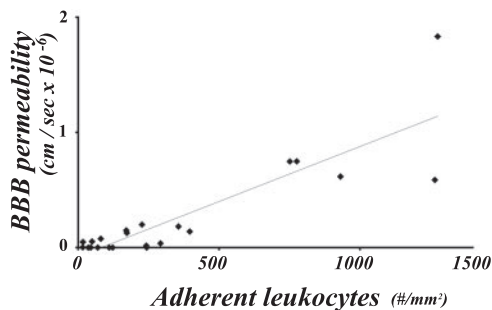


Figure 4. Relationship between leukocyte endothelial cell adhesion and BBB permeability in mice subjected to CVST ($r^2=0.75$, n=22).

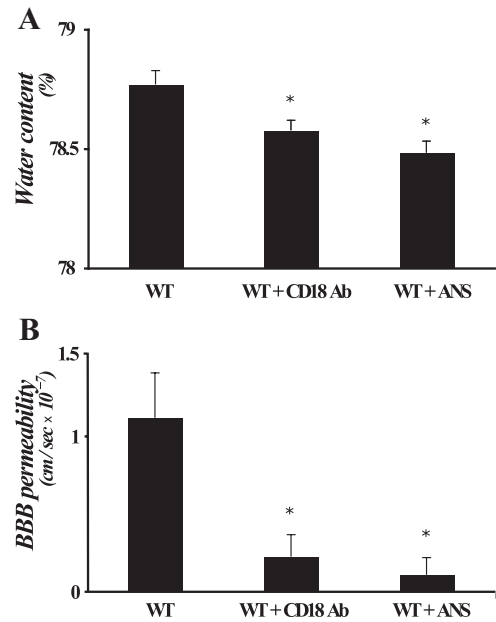


Figure 5. Effects of CD18 immunoneutralization (CD18Ab) and neutropenia (ANS) on brain responses to CVST at 48 hours. WT mice were exposed to CVST induction (by FeCl₃) 48 hours before the measurements, but without any treatment. In WT-cont, WT+CD18Ab, WT+ANS, n=8, 6, 5, respectively in A, whereas n=6, 6, 5 in B. *P<0.05 vs WT.

with leukocyte adhesion or rendering mice neutropenic altered the development of brain edema and increased BBB permeability at 48 hours after induction of CVST (Figure 5). These experiments indicate that both CD18 immunoneutralization and neutropenia were effective in reducing CVST-induced brain edema (Figure 5A) as well as the BBB dysfunction (Figure 5B).

Discussion

A major life-threatening consequence of CVST is cerebral edema.²⁷ The edema is believed to result from an elevated intravascular pressure that occurs secondary to sinus thrombosis, with the combination of an increased capillary hydrostatic pressure and pressure-induced BBB disruption directly mediating the brain swelling. In view of the extensive collateral circulation in the cerebral venous system, it is possible that other mechanisms may also account for the responses to CVST. In this study, we provide evidence suggesting that inflammatory cell recruitment, linked to an impaired PC pathway, contributes the edemagenic responses to CVST.

Previous studies have demonstrated brain edema, increased BBB permeability and intracranial pressure, and neutrophil infiltration in rodent models of CVST.^{4-6,28} Some CVST models have yielded evidence for significant perfusion deficits in the brain,²⁹⁻³¹ leading to speculation that the pathogenesis of CVST may parallel that of ischemic stroke. However, measurements of cerebral blood flow in our mouse model of CVST revealed small and seemingly inconsequential changes in brain perfusion, especially when compared to the 90% reduction in brain perfusion during occlusion of the middle cerebral artery in mice.³² Despite the unaltered brain perfusion, we detected significant brain edema, as well as

increased BBB permeability and leukocyte-endothelial cell adhesion at 48 hours following the induction of CVST. At 3 hours after CVST, there was no evidence for edema or BBB disruption, but increased leukocyte adhesion with elevated MCP-1 and lower IL-10 concentrations in brain tissue were detected, suggesting that the tissue assumes an inflammatory phenotype prior to the edemagenic response.

APC has been shown to exert significant antiinflammatory and neuroprotective effects in animal models of ischemic and hemorrhagic stroke.^{11,13–15,18–20} Here, we provide evidence that implicates APC in the inflammation and edemagenic responses to experimental CVST. Overexpression of EPCR conferred protection against the leukocyte recruitment, BBB disruption, and brain edema elicited by CVST, whereas immunoblockade of endogenous APC produced the opposite responses.

Several previous studies have demonstrated a link between increased vascular permeability and leukocyte-endothelial cell adhesion.^{33,34} Our CVST model revealed a significant positive correlation between BBB permeability and the number of adherent leukocytes, suggesting that the CVST-induced BBB disruption may be dependent on the adhesion of leukocytes or vice versa. A dependency of BBB permeability on leukocyte adhesion is supported by our observations that either inhibiting leukocyte adhesion (CD18 mAb) or inducing neutropenia (ANS) largely prevented the increased BBB permeability and brain edema observed 48 hours after the induction of CVST. Although the mechanism for the barrier protective effect of APC remains unclear, our findings, coupled to the observed relationships between BBB permeability and leukocyte adhesion after CVST in animals subjected to endogenous APC manipulation, suggest that APC may exert its protective effect via modulation of leukocyte–endothelial cell adhesion. This is consistent with evidence that the APC–EPCR complex is involved in the regulation of P-selectin expression.³⁵ However, in vitro studies indicate that APC can directly blunt BBB permeability responses via PAR-1 activation,^{12,17,18} suggesting multiple modes of action of APC.

In conclusion, the results of this study provide evidence that the inflammatory and edemagenic responses in brain tissue after CVST are linked to alterations in the PC pathway and leukocyte–endothelial cell adhesion. Our findings suggest that APC or anti-leukocyte adhesion therapies may be useful in the management of CVST patients with a poor prognosis related to severe cerebral edema.

Sources of Funding

This work was supported by funds from the Malcolm Feist Cardiovascular Endowment, a grant from the National Heart Lung and Blood Institute (HL26441), and Leducq International Network Against Thrombosis (LINAT) awarded by the Leducq Foundation, Paris. C.T.E. is an investigator of the Howard Hughes Medical Institute.

Disclosures

None.

References

- Masuhr F, Mehraein S, Einhaupl K. Cerebral venous and sinus thrombosis. *J Neurol*. 2004;251:11–23.
- Ducreux D, Oppenheim C, Vandamme X, Dormont D, Samson Y, Rancurel G, Cosnard G, Marsault C. Diffusion-weighted imaging patterns of brain damage associated with cerebral venous thrombosis. *AJNR Am J Neuroradiol*. 2001;22:261–268.
- Keller E, Flacke S, Urbach H, Schild HH. Diffusion- and perfusion-weighted magnetic resonance imaging in deep cerebral venous thrombosis. *Stroke*. 1999;30:1144–1146.
- Kim DE, Schellingerhout D, Jaffer FA, Weissleder R, Tung CH. Near-infrared fluorescent imaging of cerebral thrombi and blood-brain barrier disruption in a mouse model of cerebral venous sinus thrombosis. *J Cereb Blood Flow Metab*. 2005;25:226–233.
- Rother J, Waggie K, van Bruggen N, de Crespigny AJ, Moseley ME. Experimental cerebral venous thrombosis: Evaluation using magnetic resonance imaging. *J Cereb Blood Flow Metab*. 1996;16:1353–1361.
- Rottger C, Bachmann G, Gerriets T, Kaps M, Kuchelmeister K, Schachenmayr W, Walberer M, Wessels T, Stolz E. A new model of reversible sinus sagittalis superior thrombosis in the rat: magnetic resonance imaging changes. *Neurosurgery*. 2005;57:573–580; discussion 573–580.
- Vosko MR, Rother J, Friedl B, Bultemeier G, Kloss CU, Hamann GF. Microvascular damage following experimental sinus-vein thrombosis in rats. *Acta Neuropathol*. 2003;106:501–505.
- Esmon CT. The protein C pathway. *Chest*. 2003;124:26S–32S.
- Esmon CT. The interactions between inflammation and coagulation. *Br J Haematol*. 2005;131:417–430.
- Mosnier LO, Zlokovic BV, Griffin JH. The cytoprotective protein C pathway. *Blood*. 2007;109:3161–3172.
- Cheng T, Petraglia AL, Li Z, Thiyagarajan M, Zhong Z, Wu Z, Liu D, Maggirwar SB, Deane R, Fernandez JA, LaRue B, Griffin JH, Chopp M, Zlokovic BV. Activated protein C inhibits tissue plasminogen activator-induced brain hemorrhage. *Nat Med*. 2006;12:1278–1285.
- Domotor E, Benzakour O, Griffin JH, Yule D, Fukudome K, Zlokovic BV. Activated protein C alters cytosolic calcium flux in human brain endothelium via binding to endothelial protein C receptor and activation of protease activated receptor-1. *Blood*. 2003;101:4797–4801.
- Fernandez JA, Xu X, Liu D, Zlokovic BV, Griffin JH. Recombinant murine-activated protein C is neuroprotective in a murine ischemic stroke model. *Blood Cells Mol Dis*. 2003;30:271–276.
- Griffin JH, Zlokovic B, Fernandez JA. Activated protein C: Potential therapy for severe sepsis, thrombosis, and stroke. *Semin Hematol*. 2002;39:197–205.
- Griffin JH, Fernandez JA, Liu D, Cheng T, Guo H, Zlokovic BV. Activated protein C and ischemic stroke. *Crit Care Med*. 2004;32:S247–S253.
- Guo H, Liu D, Gelbard H, Cheng T, Insalaco R, Fernandez JA, Griffin JH, Zlokovic BV. Activated protein C prevents neuronal apoptosis via protease activated receptors 1 and 3. *Neuron*. 2004;41:563–572.
- Liu D, Cheng T, Guo H, Fernandez JA, Griffin JH, Song X, Zlokovic BV. Tissue plasminogen activator neurovascular toxicity is controlled by activated protein C. *Nat Med*. 2004;10:1379–1383.
- Lo EH. Combination stroke therapy: easy as APC? *Nat Med*. 2004;10:1295–1296.
- Shibata M, Kumar SR, Amar A, Fernandez JA, Hofman F, Griffin JH, Zlokovic BV. Anti-inflammatory, antithrombotic, and neuroprotective effects of activated protein C in a murine model of focal ischemic stroke. *Circulation*. 2001;103:1799–1805.
- Toltl LJ, Shin LY, Liaw PC. Activated protein C in sepsis and beyond: update 2006. *Front Biosci*. 2007;12:1963–1972.
- Li W, Zheng X, Gu J, Hunter J, Ferrell GL, Lupu F, Esmon NL, Esmon CT. Overexpressing endothelial cell protein C receptor alters the hemostatic balance and protects mice from endotoxin. *J Thromb Haemost*. 2005;3:1351–1359.
- Fischer S, Gerriets T, Wessels C, Walberer M, Kostin S, Stolz E, Zheleva K, Hocke A, Hippenstiel S, Preissner KT. Extracellular RNA mediates endothelial-cell permeability via vascular endothelial growth factor. *Blood*. 2007;110:2457–2465.
- Srivastava AK, Gupta RK, Haris M, Ray M, Kalita J, Misra UK. Cerebral venous sinus thrombosis: developing an experimental model. *J Neurosci Methods*. 2007;161:220–222.
- Stokes KY, Clanton EC, Bowles KS, Fuseler JW, Chervenak D, Chervenak R, Jennings SR, Granger DN. The role of T-lymphocytes in

- hypercholesterolemia-induced leukocyte-endothelial interactions. *Microcirculation*. 2002;9:407–417.
25. Gaber MW, Yuan H, Killmar JT, Naimark MD, Kiani MF, Merchant TE. An intravital microscopy study of radiation-induced changes in permeability and leukocyte-endothelial cell interactions in the microvessels of the rat pia mater and cremaster muscle. *Brain Res Brain Res Protoc*. 2004;13:1–10.
 26. Yuan H, Gaber MW, Boyd K, Wilson CM, Kiani MF, Merchant TE. Effects of fractionated radiation on the brain vasculature in a murine model: blood-brain barrier permeability, astrocyte proliferation, and ultrastructural changes. *Int J Radiat Oncol Biol Phys*. 2006;66:860–866.
 27. Lemke DM, Haccin-Bey L. Cerebral venous sinus thrombosis. *J Neurosci Nurs*. 2005;37:258–264.
 28. Frerichs KU, Deckert M, Kempfski O, Schurer L, Einhaupl K, Baethmann A. Cerebral sinus and venous thrombosis in rats induces long-term deficits in brain function and morphology—evidence for a cytotoxic genesis. *J Cereb Blood Flow Metab*. 1994;14:289–300.
 29. Miyamoto K, Heimann A, Kempfski O. Microcirculatory alterations in a mongolian gerbil sinus-vein thrombosis model. *J Clin Neurosci*. 2001;8 Suppl 1:97–105.
 30. Nakase H, Sakaki T, Kempfski O. A scanning technique to measure regional cerebral blood flow and oxyhemoglobin level. *Neurosurgery*. 2001;48:1335–1342; discussion 1342–1333.
 31. Ueda K, Nakase H, Miyamoto K, Otsuka H, Sakaki T. Impact of anatomical difference of the cerebral venous system on microcirculation in a gerbil superior sagittal sinus occlusion model. *Acta Neurochir (Wien)*. 2000;142:75–82.
 32. Yilmaz G, Arumugam TV, Stokes KY, Granger DN. Role of T lymphocytes and interferon-gamma in ischemic stroke. *Circulation*. 2006;113:2105–2112.
 33. Gavins F, Yilmaz G, Granger DN. The evolving paradigm for blood cell-endothelial cell interactions in the cerebral microcirculation. *Microcirculation*. 2007;14:667–681.
 34. Zhu L, He P. Fmlp-stimulated release of reactive oxygen species from adherent leukocytes increases microvessel permeability. *Am J Physiol Heart Circ Physiol*. 2006;290:H365–H372.
 35. Bezuhly M, Cullen R, Esmon CT, Morris SF, West KA, Johnston B, Liwski RS. Role of activated protein c and its receptor in inhibition of tumor metastasis. *Blood*. 2009;113:3371–3374.